Computation of Homoclinic Solutions to Periodic Orbits in a Reduced Water-wave Problem

A.R. Champneys and G.J. Lord
Department of Engineering Mathematics
University of Bristol
Bristol, U.K.
BS8 1TR

Revised Version June 1996

Abstract

This paper concerns homoclinic solutions to periodic orbits in a fourth-order Hamiltonian system arising from a reduction of the classical water-wave problem in the presence of surface tension. These solutions correspond to travelling solitary waves which converge to non-decaying ripples at infinity. An analytical result of Amick and Toland, showing the existence of such homoclinic orbits to small amplitude periodic orbits in a singular limit, is extended numerically. Also, a related result by Amick and McLeod, showing the non-existence of homoclinic solutions to zero, is motivated geometrically. A general boundary-value method is constructed for continuation of homoclinic orbits to periodic orbits in Hamiltonian and reversible systems. Numerical results are presented using the path-following software AUTO, showing that the Amick–Toland solutions persist well away from the singular limit and for large-amplitude periodic orbits. Special account is taken of the phase shift between the two periodic solutions in the asymptotic limits. Furtermore, new multimodal homoclinic solutions to periodic orbits are shown to exist under a transversality hypothesis, which is verified *a posteriori* by explicit computation. Continuation of these new solutions reveals limit points with respect to the singular parameter.

1 Introduction

The aim of this paper is to present numerically new generalised solitary wave solutions of a model relevant in the study of water waves and in so doing to demonstrate a more general numerical method for the continuation of homoclinic solutions to periodic orbits in Hamiltonian systems.

Direct numerical methods for computing orbits homoclinic to equilibria in continuous-time dynamical systems have been of much interest recently; see Beyn (1990), Friedman & Doedel (1991), Champneys & Kuznetsov (1994) and references therein. The key idea is to use the linearisation at the equilibrium to define boundary conditions giving the correct asymptotic behaviour for a solution over a truncated interval. These methods can readily be extended to Hamiltonian systems where, generically homoclinic orbits are a codimension zero phenomenon, that is, they persist as a parameter is varied. The technique suggested by Beyn (1990, p.385), which is the one adopted here, is to introduce an artificial Hamiltonian-breaking parameter, so that the problem becomes a codimension-one problem.

A related numerical problem is that of continuation of homoclinic solutions to periodic orbits, that is, solutions which are asymptotic to the same periodic solution in forwards and backwards time (up to a suitable phase shift). Such a connecting orbit is of codimension zero for non–Hamiltonian dynamical systems and may be computed as a homoclinic orbit to a fixed points of a Poincaré or time-τ map (Bai, Lord & Spence 1995), or by computing the periodic orbit and its linearisation in tandem with the homoclinic orbit. The well-posedness of this latter approach was shown by Beyn (1994), although he only constructed an explicit algorithm for the case of an equilibrium-to-periodic connecting orbit.

The present paper considers the special case of Hamiltonian systems for which there exist one-dimensional continuum of periodic orbits of saddle type (that is, having a stable and an unstable manifold both of the dimension equal to the number of degrees of freedom of the system). The existence of a homoclinic solution to any given orbit among this continuum is then generically of codimension zero. In Section 3 below, we propose a computational method for this problem based on the approach of Beyn (1994).

Homoclinic orbits often arise as spatially localised similarity solutions to partial differential equations. Classical examples of such are traveling solitary gravity-capillary waves on the free surface of a two-dimensional fluid subject to surface tension. Various approximations to this problem lead to Korteweg-de Vries (KdV) type equations (e.g. Craig & Groves (1994)) which have famous soliton solutions. In a co-ordinate frame that travels at the wave-speed, these solutions correspond to homoclinic orbits to an equilibrium of an ordinary differential equation. In recent years there has been much progress on rigorous results concerning solutions to the exact formulation of the water wave problem in the presence of surface tension, using a centre-manifold reduction of the Euler equation and a free-surface condition; see, for example, (Kirchgassner 1988, Amick & Kirchgassner 1989, Iooss & Kirchgassner 1992, Buffoni, Groves & Toland 1995). In the parameter plane of Froude number (measuring wave-speed) versus Bond number (measuring surface tension), one can identify certain curves, corresponding to degeneracies in the spectrum, and low-order Hamiltonian systems that are normal-forms near these curves. The aim of the centre-manifold analysis is to show that certain solutions to these low-order models persist for the full water-wave problem. For example in Buffoni et al. (1995) it is shown that homoclinic solutions to zero of a simple fourth-order equation (obtained by changing the signs of the final two terms of (1.1) below) correspond to solitary water-waves for a

horn of Bond and Froude numbers greater than 1/3 and 1 respectively. In Champneys & Toland (1993) and Buffoni, Champneys & Toland (1994) existence was shown for this equation of infinitely many *multi-modal* or *N-homoclinic* solutions, that is, waves consisting of several, N, large bumps connected by arbitrary numbers of small oscillations and with *exponentially decaying oscillations* in their tails. See, for example, (Belyakov & Shil'nikov 1990, Haller & Wiggins 1995, Sandstede 1993, Homburg, Kokubu & Krupa 1994) for N-homoclinic orbits arising in other contexts. Numerical work has shown the global bifurcation diagram of these solutions to be highly complex (Buffoni et al. 1994). Recently, Dias, Menasce & Vanden-Broek (1995) have computed certain multi-modal solutions for the full water-wave problem in finite and infinite depth, using a boundary integral method.

The problem of concern here is that of homoclinic orbits to periodic orbits of a fourth-order equation (1.1) which corresponds to Bond numbers less than 1/3 and Froude numbers greater than 1. No rigorous centre-manifold results proving the persistence of solutions of problem in the full water-wave problem is known so far. However, solitary-wave solutions with ripples at infinity do exist in this parameter regime for the full problem (Beale 1991, Sun 1991, Iooss & Kirchgassner 1992, Lombardi 1992).

Specifically, we study the equation

$$\varepsilon^2 U^{iv}(x) + U''(x) - U(x) + U(x)^2 = 0, \quad x \in \mathbb{R}, \tag{1.1}$$

which can easily be shown to be equivalent to a fourth-order Hamiltonian system, with total energy given by

$$H = \varepsilon^2 U' U''' + \frac{U'^2}{2} - \frac{\varepsilon^2}{2} U''^2 - \frac{U^2}{2} + \frac{U^3}{3}. \tag{1.2}$$

Formally, (a scaling of) (1.1) may be derived by setting to zero a first integral of the fifth-order KdV equation

$$u_t + 6uu_x + u_{xxx} + \delta^2 \, u_{xxxxx} = 0 \tag{1.3}$$

under the assumption of traveling waves $u(x,t) = U(x - ct)$. Equation (1.3), and consequently (1.1) was derived by Hunter & Scheurle (1988) as a model for the water-wave problem in the parameter region of interest here. Boyd (1991) computed (for fixed parameter values) uni-modal homoclinic orbits to periodic orbits for traveling waves of (1.3), which solutions were given the name *weakly non-local solitary waves*. He also computed *periodic* solutions which are similar in appearance to the multi-modal homoclinic solutions presented below. Boyd also refers to several physical contexts in which the weakly non-local solitary waves are of importance. We mention finally recent asymptotic analysis by Grimshaw and co-workers showing solitary waves with oscillations at infinity for (1.3) and the nonlinear Schrödinger equation (Grimshaw 1995*a*, Grimshaw 1995*b*, Grimshaw & Joshi 1995); Akylas & Yang (1995) calculated similar solutions for a forced KdV equation.

The present work is motivated by the rigorous results of Amick & Toland (1992) for (1.1) which are related to Beale's results for the full water-wave problem. Specifically,

Amick and Toland show that given any $\varepsilon \in (0, \varepsilon_0)$, where ε_0 is sufficiently small, there exists a continuum, which may be regarded as a semi–circle in an appropriate function space. of periodic orbits of (1.1). They then prove that for any ε sufficiently small, there exist non-trivial intersections between the stable and unstable manifolds of certain of these periodic orbits of exponentially small amplitude as $\varepsilon \to 0$. The method of proof (explained in more detail in Section 2, below) shows that the solutions forming this intersection are even solutions which resemble a perturbation of $(3/2)\mathrm{sech}^2(x/2)$ by a periodic orbit (the reader may care to look ahead to Fig. 6). Note, however, the seemingly paradoxical result that despite the existence of homoclinic solutions to periodic orbits of arbitrarily small amplitude, there do not exist solutions of (1.1) homoclinic to the zero solution for small ε (Amick & McLeod 1991), moreover, there do not exist even homoclinic solutions to zero for any $\varepsilon \neq 0$.

The contribution of the present paper is to show numerically that the solutions shown to exist by Amick and Toland can be extended both up to large ε and to solutions homoclinic to large-amplitude periodic orbits. In so doing a schematic plot is produced clarifying the two-parameter bifurcation diagram of ε versus amplitude of periodic orbit (Fig. 18). We also show that there exist multi-modal versions of these orbits. That is, waves with several large bumps which are asymptotic to periodic waves at infinity (for an example see Fig. 12, below).

The rest of the paper is outlined as follows. In Section 2 we give an overview of the results of (Amick & Toland 1992), and discuss other analytical considerations for (1.1) including the non-existence of homoclinic solutions to zero and the existence of multi-modal homoclinic orbits to periodic orbits. In Section 3, we describe our numerical methods within the general context of continuation of homoclinic orbits to periodic orbits of Hamiltonian systems. In Section 4, numerical results specific to equation (1.1) are presented. Finally, in Section 5 we draw conclusions and suggest future work.

2 Analytical Results

This section concerns what is known analytically about homoclinic solutions of equation (1.1). First we review the results of Amick and Toland concerning solutions homoclinic to small-amplitude periodic orbits. The reason for including such a review is that, in the numerical investigation to follow, we construct initial approximations using the specific solutions they construct. Next, we motivate the result by Amick and McLeod on the non-existence of homoclinic orbits to the zero solution for small finite ε, by considering ideas of codimension and by performing some simple numerical experiments using shooting. Finally in this section, we present a simple argument based on transversality to show that generically, given the existence of a homoclinic orbit to a periodic solution, there will be infinitely many other multi-modal orbits to the same periodic orbit. Note that these orbits, whose existence is backed up by numerical computations in Section 4, are complimentary to those proved to exist Amick and Toland which are all uni-modal.

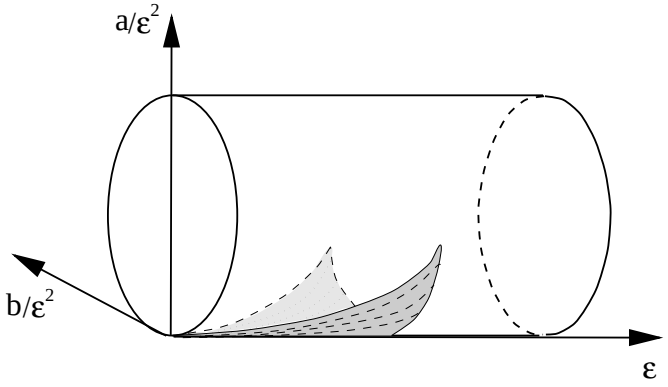

Figure 1: The cylinder of periodic solutions to (1.1) in phase–parameter space. The solutions with negative b are a phase shift of those with positive b. The shaded region represents the subset of these orbits which may posses homoclinic connections. Curves within the shaded region represent lines of constant phase-shift p according to Theorem 2.1.

2.1 The Theory of Amick and Toland

Amick & Toland (1992) commence by proving, for small ε, the existence of a set of small-amplitude, even periodic solutions of the singularly perturbed problem (1.1). In particular they look for τ-periodic solutions U of the form

$$\varepsilon^2 U(x) = a + b\cos\left(\frac{2\pi}{\tau}\,x\right) + \psi(x) \tag{2.1}$$

where τ is close to $2\pi\varepsilon$ and a and b are constants and $\psi(x)$ is small. The Implicit Function Theorem is used to show that if

$$a \in \left(0, \varepsilon^2\right) \text{ and } b \in (-\Gamma\varepsilon^2, \Gamma\varepsilon^2), \tag{2.2}$$

$$a^2 - a\varepsilon^2 + \frac{1}{2}b^2 + b^4 I(2a - \varepsilon^2, b^2, \Lambda) = 0, \tag{2.3}$$

$$\Lambda^2 - \Lambda + 2a - \varepsilon^2 + b^2 J(2a - \varepsilon^2, b^2, \Lambda) = 0, \tag{2.4}$$

where $\Lambda = \frac{4\pi^2\varepsilon^2}{\tau^2}$, for some constant Γ and smooth functions I, J, then ψ is determined uniquely by a and b. In fact, it is shown that even solutions to (1.1) of the form (2.1) lie on a cylinder in (a, b, ε)-space, which implies that, for each $\varepsilon > 0$, there exists a circle of even periodic orbits in the phase space of equation (1.1) with the amplitude of the periodic solution parametrised by b (see Fig. 1). More accurately, there is a semi-circle of distinct even periodic orbits, because the orbits with negative b are related to those with positive b by translation through half a period. Also, the top and bottom of the circle, corresponding to $a = \varepsilon^2, b = 0, \psi = 0$ and $a = 0, b = 0, \psi = 0$, represent the two equilibria $U \equiv 1$ and $U \equiv 0$ respectively.

In what follows the phase of the periodic solution is crucially important. To that end, we let $U(x) = \Phi_b^\varepsilon(x)$ be the τ–periodic solution of (1.1) parametrised by b and ε such that $U'(0) = 0$ and $U''(0) < 0$ and let

$$\Phi_{b,p}^\varepsilon(x) = \Phi_b^\varepsilon(x - p\tau), \qquad p \in [0, 1) \tag{2.5}$$

denote the shift through $p\tau$.

Now recall that the equation $\sigma'' - \sigma + \sigma^2 = 0$, is satisfied by the function

$$\sigma(x) = \frac{3}{2}\mathrm{sech}^2\left(\frac{x}{2}\right), \quad x \in \mathbb{R}.$$

To prove the existence of a homoclinic orbit to a periodic orbit for (1.1) Amick and Toland seek an even solution $U(x)$ of (1.1) of the form

$$U(x) = \sigma(x) + \Phi_{b,p}^\varepsilon(x) + \omega(x), \qquad x > 0, \qquad \omega(x) \to 0 \ \text{ as } \ x \to \infty. \tag{2.6}$$

Such a solution is asymptotic to $\Phi_{b,p}^\varepsilon(x)$ as $x \to \infty$ and, due to its evenness, to $\Phi_{b,-p}^\varepsilon(x)$ as $x \to -\infty$. The proof of the following theorem constitutes Section 3 of (Amick & Toland 1992) and indeed the greater part of that paper.

Theorem 2.1 *For every given phase $p \in [0, 1/2)$, there exists $\varepsilon_p > 0$ and a positive constant $C = C(p)$, independent of $\varepsilon \in (0, \varepsilon_p)$ such that*

1. *there exists an even solution to* (1.1) *of the form* (2.6) *with $b = b(\varepsilon)$,*
2. *$\|\omega\| \le C\varepsilon^2$,*
3. *for each N there exists a constant K such that*

$$\left|b(\varepsilon)/\varepsilon^2\right| \le K\varepsilon^N, \quad \text{as} \qquad \varepsilon \to 0.$$

By construction, the *phase-shift* $P_H \in [0, 1)$ [1] between the two periodic solutions in the limits $x \to \pm\infty$ for a homoclinic orbit is given by

$$P_H = 2p. \tag{2.7}$$

It should be noted that the case of zero phase-shift, $P_H = 0$ was a special case in the proof of the theorem, requiring quite different estimates.

The consequence of this theorem is then that given any phase-shift there exists a homoclinic solution to a periodic orbit within an exponentially thin wedge of the cylinder in parameter space (see Fig. 1). Note that, for a fixed ε and phase-shift, the proof of the theorem shows local but not global uniqueness of homoclinic orbits. Therefore other solutions may exist for the same phase-shift and the same value of ε, which are homoclinic to periodic orbits in the unshaded region of the cylinder. Moreover, the local uniqueness

[1] we henceforth refer to phase-shift as being measured by a fraction of the period

is for fixed phase p, not for a fixed periodic orbit, hence there may be more than one homoclinic solution to any given periodic orbit.

The homoclinic solutions proved to exist are all uni-modal, as in Fig. 6. Moreover they are even solutions, which implies that these solutions in the corresponding four-dimensional phase space are invariant under the reversibility transformation

$$R : (U, U', U'', U''') \to (U, -U', U'', -U''') \quad \text{and} \quad x \to -x, \tag{2.8}$$

which necessarily implies $U'(0) = U'''(0) = 0$. The possibility of solutions which are not invariant under the reversibility will concern us later.

Finally, note the numerical observation that for any given ε sufficiently small, each member of the family of periodic orbits $\Phi_b^\varepsilon(x)$ has a different value of the Hamiltonian H. Hence, each member of the continuum of homoclinic solutions shown to exist by Theorem 2.1 generically exists within the level surface corresponding to an isolated H-value, so that the family may be locally parametrised by the value of H.

2.2 Homoclinic Orbits to Zero

One could easily be lead to believe that, because Theorem 2.1 gives the existence of homoclinic solutions to periodic orbits of arbitrarily small amplitude, then, continuity must lead to the existence of homoclinic orbits to the zero solution of (1.1). However, this line of reasoning is false, because Amick & McLeod (1991) have proved that there are no even homoclinic solutions to zero for (1.1) for any $\varepsilon > 0$ and for ε sufficiently small that no orbits homoclinic to zero exist. Although at first sight they seem paradoxical, these results are not so surprising when one considers the codimension of the intersections required of the appropriate stable and unstable manifolds in the four-dimensional phase space (U, U', U'', U'''), as we now discus.

Each periodic solution proved to exist by Amick and Toland has stable and unstable manifolds of dimension two. The existence of a homoclinic solution to this periodic orbit occurs when these two two-dimensional manifolds intersect along a line. Within a level set of the Hamiltonian function $H =$ constant, such an intersection, if transverse, would clearly be structurally stable; see Fig. 2. Therefore, we generically expect homoclinic solutions to periodic orbits to persist as we vary ε.

In contrast, consider now the equilibrium at the origin. We note that for non-zero ε it is always a saddle-centre with eigenvalues $i\alpha, -i\alpha, \beta, -\beta$, for some $\alpha(\varepsilon), \beta(\varepsilon) > 0$. Furthermore, we know that its centre manifold locally consists of a one-parameter family of periodic orbits.

Therefore, if a homoclinic solution to the equilibrium exists it must be contained in both the one-dimensional stable and unstable manifolds. Thus we require that one component of the unstable manifold must be identified with a component of the stable manifold (see Fig. 3). This is clearly not structurally stable, even within the zero level set of H. Thus we do not expect such solutions to exist other than for isolated values of ε. Moreover, in the special case of even solutions, for a homoclinic solution we require an intersection between the unstable manifold W^u and the symmetric section

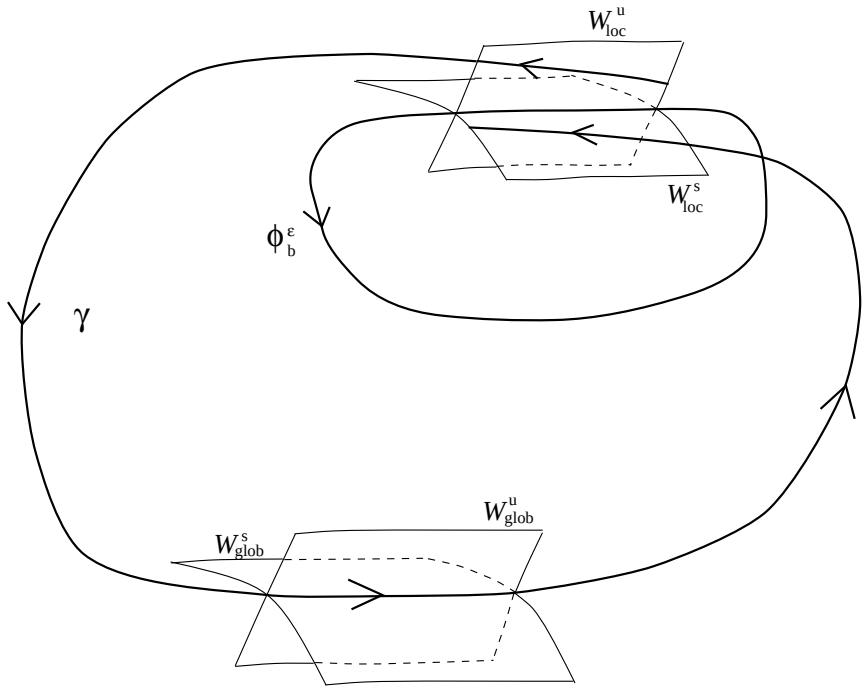

Figure 2: Depicting a homoclinic orbit to a periodic orbit as a transverse intersections of the stable (W^s) and unstable (W^u) manifolds in the three dimensional phase space H =const. In the picture, W^u_{glob} is the forward image of the local unstable manifold W^u_{loc} around the homoclinic orbit γ whereas W^s_{glob} is the backwards image of W^s_{loc}.

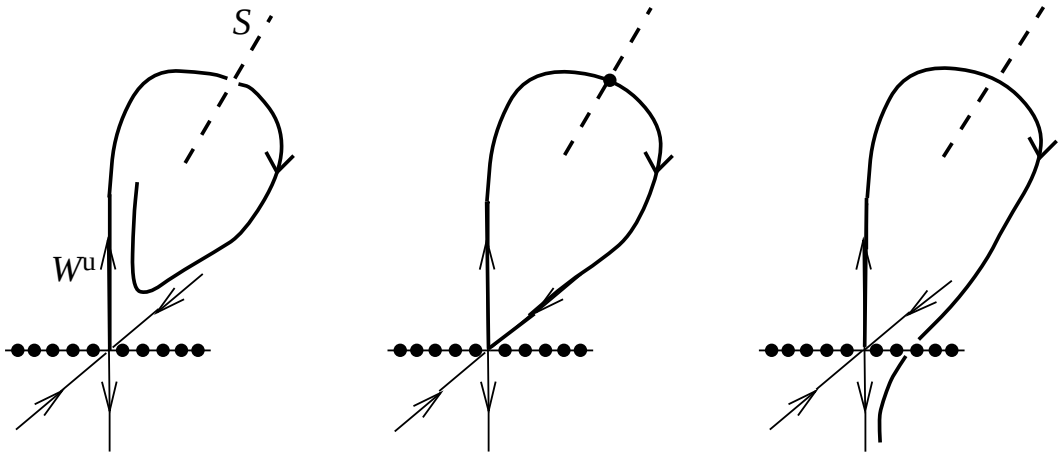

Figure 3: Showing how generic perturbations would break homoclinic orbits to the origin. The figure is drawn in three-dimensions by projecting out one direction tangent to the centre manifold, on which periodic orbits are represented by solid dots. The line S represents the intersection of the symmetric section with the zero level set of H.

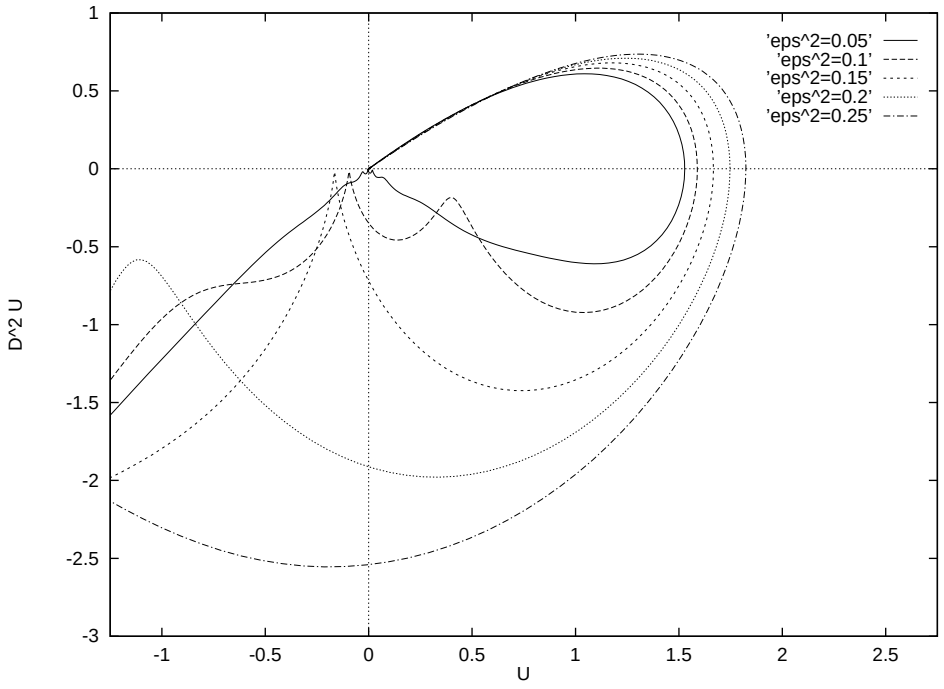

Figure 4: Numerical computation of one component of the unstable manifold of the origin of (1.1), projected onto the (U, U'')-plane, for a range of values of ε^2 between 0.05 and 0.25

$\mathcal{S} = \{U, U', U'', U''' \mid U' = U''' = 0\}$ and, because W^u and $\mathcal{S} \cap \{H = 0\}$ are both one-dimensional sets, we conclude that the existence of an even homoclinic orbit to zero is of codimension one[2]. Since we know that such a solution exists at $\varepsilon = 0$, it would therefore seem reasonable to find no solutions for small ε. To illustrate this, the behaviour of the component of the unstable manifold which forms the solution $(3/2)\mathrm{sech}^2(x/2)$ at $\varepsilon = 0$ has been computed numerically for non-zero ε. The results are plotted in Fig. 4, projected onto the (U, U'')-plane, which shows that as ε increases the unstable manifold returns further and further away from the origin and escapes to infinity in the third quadrant. Further numerical experiments indicate that this qualitative behaviour persists for all $\varepsilon > 0$.

Note finally, that given a *two*-parameter problem, we would expect homoclinic orbits to zero, if they exist, to occur along isolated lines in the parameter plane. Hence the existence or otherwise of such solutions for the full water-wave problem remains an open question.

[2]Homoclinic orbits to zero that are not symmetric under the reversibility, will generically be of codimension two (Koltsova & Lerman 1995).

2.3 Multi-modal Homoclinic Orbits to Periodic Orbits

We now argue that generically, given any homoclinic orbit formed by the transverse intersection of the stable and unstable manifolds of any saddle-type periodic orbit Φ_b^ε of (1.1), there must be infinitely many other multi-modal homoclinic orbits to the same periodic orbit Φ_b^ε.

Note that since the system (1.1) is Hamiltonian we may restrict the dynamics to the level set of the Hamiltonian function, H = constant. In particular we may choose a value of H corresponding to the periodic orbit Φ_b^ε. This reduces the dimension of the system by one. By taking a Poincaré section Π through the periodic orbit, we can further reduce the problem to a two-dimensional map. See Fig. 5. The fixed point of the map corresponding to the periodic orbit Φ_b^ε has a one-dimensional stable and one-dimensional unstable manifold. A transverse intersection of these two 1D manifold, indicated by hollow circles in the figure, implies, via the Smale-Birkoff Homoclinic Theorem (see, e.g. Guckenheimer & Holmes (1983, Thm. 5.3.5)) the existence of chaotic dynamics. Moreover, there must exist a classical homoclinic tangle which necessarily contains infinitely many secondary intersections between the stable and unstable manifolds. One such orbit is indicated by bold dots in Fig. 5, and corresponds to an orbit that goes approximately twice around the loop represented by the original homoclinic orbit, and hence it is a *bi-modal* orbit. It is not difficult to see from the construction of the tangle that there have to be infinitely many such bimodal orbits each having a different number of iterates near Φ_b^ε and hence a different number of oscillations between the two humps of the graph of $U(x)$. Similarly, there must be infinitely many *tri-modal* orbits, 4-modal etc. The conclusion reached is therefore qualitatively similar, albeit for different reasons, to that obtained for the fourth-order equation in Buffoni et al. (1994) concerning solutions with exponentially decaying oscillations at infinity.

The only requirement to make the above argument rigourous, is to prove that the homoclinic orbits of Theorem 2.1 do indeed represent the transverse intersection between the stable and unstable manifolds of the appropriate periodic orbit. Since transverse intersections are generic and Theorem 2.1 holds for a range of ε, we would expect this transversality to hold, but it is a non-trivial task to prove it. Note also, that the argument embodied in Fig. 5 is independent of ε or of periodic orbits among the family Φ_b^ε. Hence, for each periodic orbit for which we can prove a transverse homoclinic orbit there will be an infinite number of multi-modal homoclinic orbits.

Note finally, that we have not used symmetry to argue the existence of the multi-modal homoclinic orbits, and, in general, such orbits should include both solutions that are invariant under (2.8) (i.e. even solutions $U(x)$) and those which are not.

3 Numerical Methods

We aim to compute orbits homoclinic to periodic solutions for equation (1.1) via numerical path-following. In order to achieve this, we first present a more general method, for continuation of homoclinic orbits to periodic orbits in Hamiltonian systems. The method

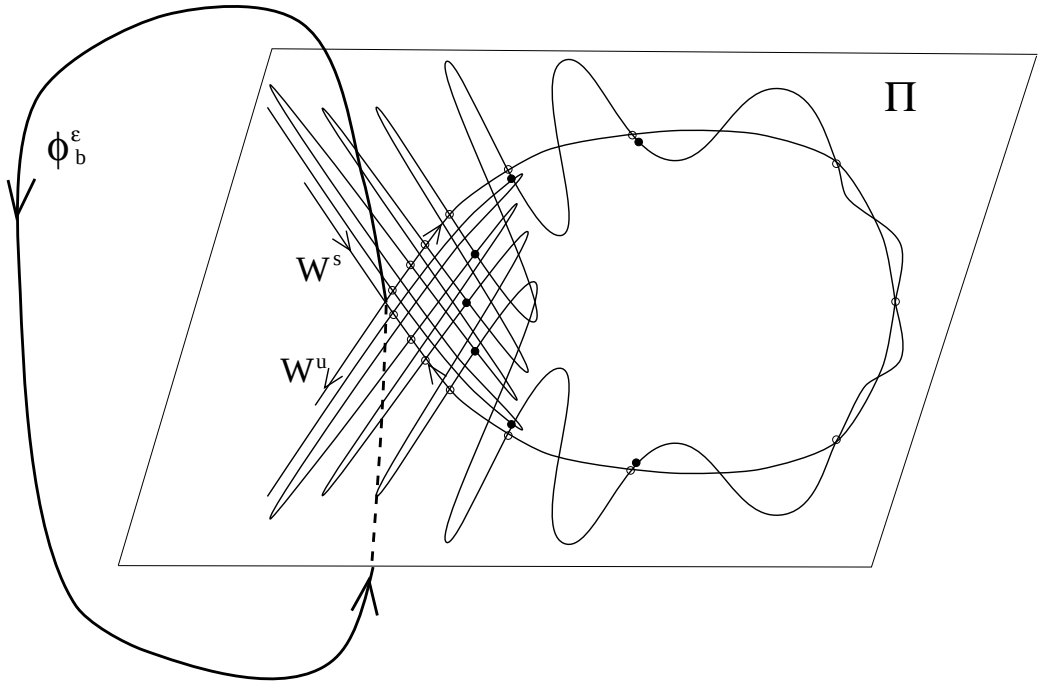

Figure 5: Representation of the intersection between the stable W^s and unstable W^u manifolds of a periodic orbit Φ_b^ε in a Poincaré section Π within a level set of the Hamiltonian.

is a modification of well-posed boundary-value approach of Beyn (1994) for computing connections between periodic solutions. In addition to solving for the homoclinic solution it is necessary also to solve for the periodic solution Φ_b^ε. Thus, essentially, we are solving two coupled 4th-order systems. For the special case of symmetric solutions under a reversibility condition, we construct a simplified method in the spirit of Champneys & Spence (1993).

3.1 A general continuation method

Consider a $2n$-dimensional smooth Hamiltonian system

$$\dot{v} = f(v(t), \mu), \quad v \in \mathbb{R}^{2n}, \quad \mu \in \mathbb{R}, \quad t \in \mathbb{R}, \tag{3.1}$$

with Hamiltonian $H(v, \mu)$, which we assume to be written in canonical variables so that

$$f(v(t), \mu) = J \nabla H(v(t), \mu),$$

where J is the usual skew-symmetric $2n \times 2n$-matrix. Suppose there exists a one dimensional continuum of periodic orbits $\phi_h(t)$ of period $\tau(h)$ that can be parametrised by the value h of H and are of saddle type (i.e. having $n-1$ stable and $n-1$ unstable Floquet multipliers). We suppose further that there exists a solution $v(t) = \gamma(t)$ that is homoclinic to $\phi_h(t)$. Finally, let $\phi_{h,p}(t)$ denote the periodic orbit with phase shifted by p, $\phi_{h,p}(t) = \phi_h(t - p\tau)$. We seek both the periodic and homoclinic orbits as solutions to an appropriate boundary-value problem.

Periodic Orbit

To write a well-posed problem for the periodic orbit $\phi_h(t)$, we introduce an artificial Hamiltonian-breaking parameter λ_1 (as in Schmidt (1976), an approximation T_P to the period of the orbit and then re-scale time so that the period becomes unity. Hence we solve

$$\dot{v} = T_P \left(J \nabla H(v, \mu) + \lambda_1 \nabla H(v, \mu) \right), \quad t \in [0, 1] \tag{3.2}$$

subject to the natural periodic boundary conditions

$$v(0) = v(1). \tag{3.3}$$

Furthermore, the Hamiltonian is constrained to be constant

$$H(v, \mu) = h, \tag{3.4}$$

and a condition imposed to fix the phase of the periodic orbit, which we write as a scalar equation

$$\Psi(v(t), T_P, \mu) = p. \tag{3.5}$$

We assume that Ψ satisfies a suitable non-degeneracy condition; a specific choice of Ψ will be discussed in Section 3.2. Note that the introduction of λ_1 is necessary in order

to make (3.2)–(3.5) a well-posed problem for the unknowns $(v(t), T_P, \lambda_1)$ with a locally unique solution $(\phi_{h,p}(t), \tau, 0)$.

Homoclinic Orbit: General Case

For the homoclinic orbit, we solve for an approximation $\hat{\gamma}$ defined over a truncated interval $[0, T_H]$, where $T_P \ll T_H$ and re-scale time. First we present a general method and then we propose a simplification specific for symmetric orbits in reversible Hamiltonian systems. In the general case we solve an extended system analogous to (3.2)

$$\dot{w} = T_H \left(J\nabla H(w, \mu) + \lambda_2 \nabla H(w, \mu) \right), \quad t \in [0, 1], \tag{3.6}$$

where λ_2 is again a Hamiltonian-breaking parameter which should be zero for the true solution. We take projection boundary conditions

$$L_s \left(w(0) - v(0) \right) = 0, \tag{3.7}$$

$$L_u \left(w(1) - v(0) \right) = 0, \tag{3.8}$$

where $v(t)$ solves (3.2)–(3.5) and the rows of the $(n+1) \times 2n$-matrices $L_{s,u}$ span the left eigenspaces corresponding to the centre-stable and centre-unstable Floquet multipliers respectively of the periodic orbit $\phi_{h,p}(t)$ at $v(0)$ (Beyn 1994). Note that both these subspaces have the two central directions $\nabla H(v(0), \mu)$ and $\dot{v}(0)$ in common. The computation of $L_{s,u}$ in general requires the solution of $2n$ variational equations of dimension $2n$ (the adjoint of the linearisation of (3.1) about $\phi_{h,p}$) with appropriate initial conditions. This greatly increases the dimension of the system to be solved. Instead, in the implementation described below, we use the monodromy matrix provided by the boundary-value solver for (3.2)–(3.5) to compute the necessary eigenspaces. Thus, to compute the homoclinic orbit we solve (3.2)–(3.5) in tandem with (3.6)–(3.8) for the unknown functions $w(x)$, $v(x)$ and free parameters $T_P, T_H, \lambda_1, \lambda_2$ and either h or μ.

Taking h to be a free parameter allows for varying the periodic orbit at a fixed parameter value, whereas taking μ as a free parameter allows continuation of solutions to a single periodic orbit as the problem parameter varies. Note that the phase shift P_H between the periodic solutions to which the homoclinic orbit is asymptotic as $t \to \pm\infty$ is given by

$$P_H = T_H \pmod{T_P}. \tag{3.9}$$

Hence, the free parameter T_H plays the role of the phase-shift parameter for this form of continuation. It should be noted that the periodic orbit and homoclinic solution are coupled only through the projection boundary conditions (3.7) and (3.8). Finally, note that we do not impose a phase condition directly on the homoclinic orbit, its phase is fixed by the phase p of the periodic orbit .

Homoclinic Orbit: Symmetric Case

We now look at the special case where (3.1) is a reversible Hamiltonian system. Specifically, we suppose that there exists an involution R, such as (2.8), under which the system

is invariant after a reversal of time and such that $\mathcal{S} = \mathrm{fix}(R)$ is an n-dimensional submanifold of the phase space $\mathbb{R}^{2n}$ (Devaney 1976). Solutions $v(t)$ which are themselves symmetric under R (such as those homoclinic orbits described by Theorem 2.1) must satisfy the n-dimensional constraint $v(0) \in \mathcal{S}$. Thus, for symmetric orbits, we can replace the right-hand boundary conditions (3.8) with

$$w(1) \in \mathcal{S}. \tag{3.10}$$

Since (3.10) is one less constraint than (3.8) we should remove one free parameter, namely λ_2. Hence, in this case, we solve

$$\dot{w} = T_H f(w(t), \mu), \quad t \in [0, 1], \tag{3.11}$$

subject to (3.7) and (3.10) for $w(t)$ in tandem with (3.2)–(3.5) for $v(t)$, with free parameters T_P, p, λ_1 and two of either T_H, h or μ. Note that the phase shift P_H for the homoclinic connection is now given by

$$P_H = 2(T_H \ (\mathrm{mod} T_P)) \tag{3.12}$$

so that $2T_H$ now plays the role of the phase-shift parameter.

Note that the boundary-value problem for the homoclinic part of the reversible case (given by (3.7), (3.10) and (3.11)) does not use the Hamiltonian structure of (3.1). Moreover, symmetric homoclinic and periodic orbits in reversible systems necessarily have similar properties to those in Hamiltonian systems; e.g. their codimensions are the same and the spectrum of the linearisation around periodic orbits must both be symmetric, see Devaney (1976). Hence, by modifying the boundary-value problem (3.2)–(3.5) for the periodic orbit, using symmetric-section boundary conditions rather than the Hamiltonian structure, it is straightforward to write down a defining boundary-value problem for homoclinic orbits in non-Hamiltonian reversible systems. Note, however, that we would need to replace the boundary condition (3.4) by another condition which parametrises periodic orbits among a one-dimensional continuum.

We do not provide here any theoretical justification of our numerical methods. Instead we refer to Beyn (1994) for some quite general theory using exponential trichotomies which should be adaptable to the case under consideration here. Error estimates as $T_H \to \infty$, such as exist for the case of connecting orbits to equilibria (Beyn 1990, Friedman & Doedel 1991, Schecter 1995) remain open.

3.2 Specific Implementation

3.2.1 Continuation

To perform numerical continuation on the eight-dimensional boundary-value problem resulting from (3.2)–(3.5), (3.10)–(3.11) (or, for the general case, (3.6)–(3.8)) we used the continuation code AUTO86 (Doedel & Kernevez 1986, Doedel, Keller & Kernevez 1991) which is able to solve quite general two-point boundary-value problems using orthogonal

collocation. With kind assistance form E. Doedel, the standard version of AUTO was adapted to make the monodromy matrix associated with the solution of the periodic problem (3.2)–(3.5) available to the user. The eigenvalues and associated eigenvectors of the transpose of this matrix were then computed using a standard linear algebra routine and those eigenvectors corresponding to eigenvalues with modulus less than or equal to unity were used to construct the matrix L_s (and L_u in the general, non-symmetric, case) at each step in the computation.

In order to apply the algorithms it was convenient to rewrite (1.1) in Hamiltonian co-ordinates. To that end, we choose

$$\left.\begin{array}{ll} p_1(x) = U'(x) & q_1(x) = \varepsilon^2 U''(x) + U(x), \\ p_2(x) = U'''(x) & q_2(x) = \varepsilon^2 U(x), \end{array}\right\} \tag{3.13}$$

with corresponding total energy H given by

$$H(p_1, p_2, q_1, q_2) = p_1\left(\varepsilon^2 p_2 + \frac{1}{2}p_1\right) - \frac{1}{2\varepsilon^2}\left(q_1 - \frac{q_2}{\varepsilon^2}\right)^2 - \frac{q_2^2}{2\varepsilon^4} + \frac{q_2^3}{3\varepsilon^6} \tag{3.14}$$

so that (1.1) takes the form of Hamilton's equations

$$\frac{\partial q_i}{\partial x} = \frac{\partial H}{\partial p_i}, \qquad \frac{\partial p_i}{\partial x} = -\frac{\partial H}{\partial q_i}, \qquad i = 1, 2.$$

It remains to comment on the choice of phase fixing condition (3.5) for the periodic orbit. Since the true phase p of the periodic orbit $\Phi^{\varepsilon}_{b,p}$ cannot easily be computed directly using the boundary-value approach, we set the first derivative of the periodic solution to be constant at $x = 0$:

$$v'(0) = p. \tag{3.15}$$

Note that p does not measure the true phase of the periodic orbit, but it is a smooth function of the phase, which is enough. To monitor the phase shift we regard P_H as a further free parameter and take a corresponding extra boundary condition representing a continuous version of (3.9) (or (3.12)):

$$\frac{T_H}{T_P} = P_H. \tag{3.16}$$

For the symmetric case, we take as symmetric section boundary conditions (3.10)

$$U'(1) = 0, \qquad U'''(1) = 0.$$

3.2.2 Initial Approximations to Solutions

In order to perform continuation using AUTO, it is necessary to compute an initial approximation to the solution. For the uni–modal homoclinic orbits described by Theorem 2.1, we were able to exploit the specific form of the solutions given in Section 2.1. For an approximate periodic solution of (1.1), we took the analytical form (2.1) with $\psi(x) = 0$,

and a and b approximated as follows. We first fix ε and set $a = \varepsilon^2/\nu$, where ν is an artificial parameter used to parametrise the circle of periodic orbits in Fig. 1. The period τ and b are then determined by solving the approximation to equations (2.2–2.4) defined by setting $I = J \equiv 0$, to obtain

$$a = \frac{\varepsilon^2}{\nu}, \quad b = \sqrt{2a(\varepsilon^2 - a)}, \quad \text{and} \quad \tau = \frac{2\pi\varepsilon}{0.5 + \sqrt{0.25 - 2a + \varepsilon^2}.}$$

To approximate the homoclinic solution we used the expression (2.6), using $\sigma(x) = (3/2)\mathrm{sech}^2(x/2)$, the above approximation to $\Phi^{\varepsilon}_{b,p}(x)$ and with $\omega(x)$ set to zero. Recall from Theorem 2.1, that if the periodic orbit were exact, the error in this approximation satisfies $\|\omega\| \leq C\varepsilon^2$. Note that this approximation is valid in the limit $\nu \to \infty$, which corresponds to the zero-amplitude limit. For $\varepsilon^2 = 0.01$ a value of $\nu = 1000$ proved sufficient for AUTO to converge.

For the projection boundary conditions (3.7) (or (3.8)) we are required either to compute the centre-stable (or centre-unstable) directions corresponding to the initial point on the periodic solution, or to use an approximation. Our starting computation assumed that the periodic orbit was sufficiently small (corresponding to large ν) and that the centre-stable (or centre-unstable) eigenspaces at the equilibrium could be used to approximate those of the periodic orbit until AUTO had computed the more accurate approximate directions. The eigenspaces were computed by simple linear algebra applied to the Jacobian of (1.1) at $U = 0$.

For multi–modal solutions initial approximations to solutions were found using a shooting technique similar to that used in Champneys & Spence (1993) for homoclinic orbits to equilibria. A point was chosen on the periodic orbit — using data, for example, from a previous run of AUTO. Similarly, the direction associated with the unstable Floquet multiplier at this point was either found from a previous run of AUTO or (for small amplitude periodic orbits) approximated by the unstable eigenspace of the equilibrium at zero. Approximations to the unstable manifold were then computed by solving an initial value problem starting at a variable distance along this unstable direction. Allowing this distance to vary, searching procedures were then used in order to find a homoclinic orbit.

4 Numerical Results

This section presents numerical results for the reduced water-wave problem (1.1) found using the techniques described in Section 3. In order to avoid encountering the singular limit directly, all computations in which ε vary were carried using the continuation parameter

$$\eta = 1/\varepsilon^2.$$

All continuation is performed for symmetric homoclinic connections using the algorithm described in the previous section. That is we solve (3.2) and (3.11) subject to (3.3)–(3.5) and (3.7),(3.10) respectively. For continuation with fixed Hamiltonian h the

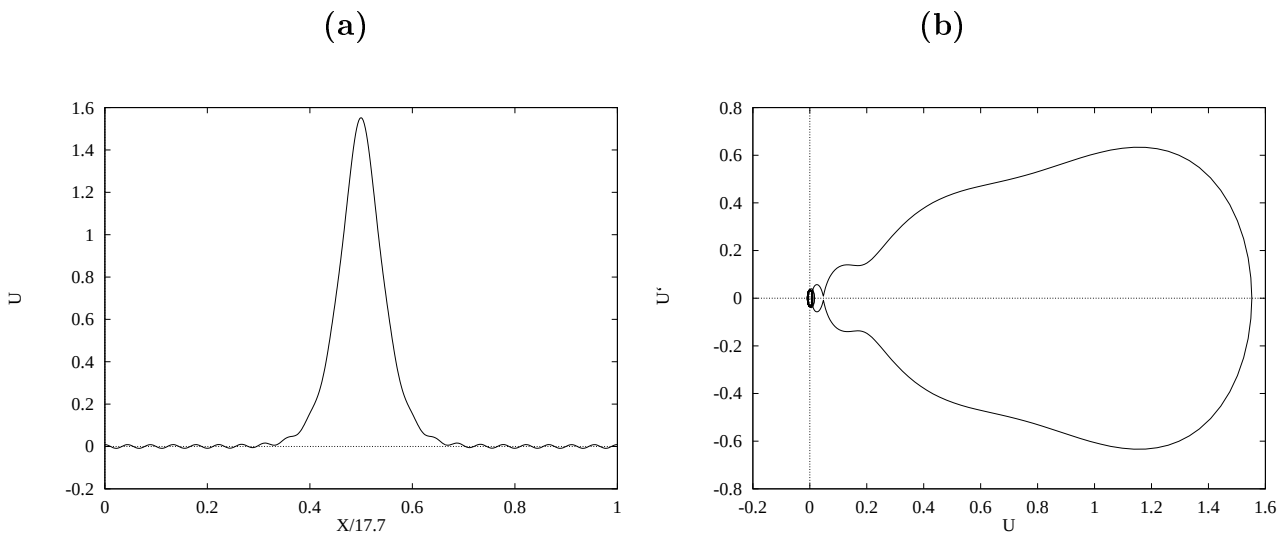

Figure 6: A homoclinic orbit to a small-amplitude periodic orbit for $1/\varepsilon^2 = 15.0$, $P_H = 0.25$ and $H = -6.48 \times 10^{-3}$. (a) Solution $U(x)$ plotted against x, (b) the same solution as $U'(x)$ plotted against $U(x)$.

free parameters were ε, T_H, T_P and λ_1. For continuation with fixed phase T_H/T_P the free parameters were ε, h, T_P and λ_1. In both these cases ε is treated as the continuation parameter. For continuation at a fixed value of ε the free parameters were T_H, T_P, h and λ_1. In this case the phase shift T_H/T_P is treated as the continuation parameter.

4.1 Uni-modal solutions

We first present the results of the numerical computation of homoclinic solutions to small-amplitude periodic orbits, of the form proved to exist in Theorem 2.1. An example of such a solution may be seen in Fig. 6 for $\eta = 15$ and a value of the Hamiltonian (3.14) of $H = 6.84 \times 10^{-4}$. Fig. 6(a) depicts the solution as a graph of $U(x)$ over a full x-interval (despite the fact that the solution was computed only over the half-interval up to the point of symmetry). Fig. 6(b) shows the solution in the plane $(U(x), U'(x))$ - corresponding to a projection of the four-dimensional phase space. It should be noted that there is nothing special about this value of ε, although care has to be taken to avoid computing spurious solutions for ε close to zero, the solution at the presented values of H and ε were chosen only for reasons of clarity.

Given homoclinic solutions to small-amplitude periodic orbits, we next show that homoclinic connections may be continued numerically up to large amplitude periodic orbits, far away from where the analysis of Amick and Toland may be expected to hold. In order to do this we fix ε and allow the value of H (parametrising the amplitude of the periodic orbit) and P_H (parametrising the the phase-shift) to vary. The results of such a computation for $1/\varepsilon^2 = 10$ is shown in Fig. 7, which shows solutions on a continuous branch plotted over the half-interval (at the right-hand end point, the symmetric section boundary conditions (3.10) are imposed). Fig. 7(a) shows three solutions plotted as graphs

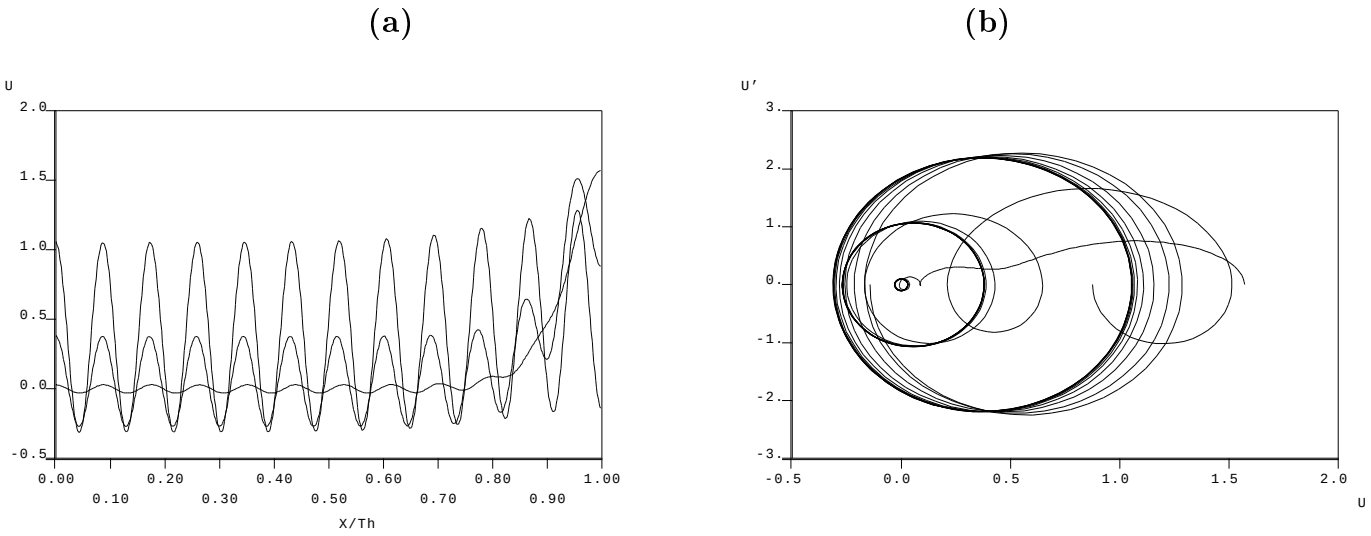

Figure 7: Continuation in phase-shift for $1/\varepsilon^2 = 10.0$. (a) Three different solutions $U(x)$ plotted against x, (b) the same solutions with $U'(x)$ plotted against $U(x)$.

of $U(x)$, Fig. 7(b) shows these solutions plotted in a projection of phase space.

The corresponding locus of solutions is represented in Fig. 8(a), showing phase-shift versus the amplitude of the periodic orbit $\Phi_b^\varepsilon(x)$ (measured by its maximum value). Recall from (3.12) that the phase-shift is measured by twice the non-integer part of T_H/T_P. The solutions depicted in Fig. 7 occur on one of the limbs of the U-shaped curve of Fig. 7(a); solutions on the other limb are similar. Note that as we follow solutions up the near-vertical part of the curve, the homoclinic orbit becomes an increasingly weaker modulation of the periodic orbit whose amplitude is rapidly growing. In the limit, at the top of each limb, the modulation disappears and the former homoclinic orbit becomes a pure large-amplitude periodic solution (the near circular orbit in Fig. 7(b)). That is in a Poincaré section each homoclinic point tends to the periodic orbit. Note that such large amplitude solutions necessarily have zero phase-shift, i.e. $T_H/T_P = 11.0$ or 11.5). It can be observed from Fig. 8(a) that the numerics has difficulty in reaching precisely these two limits, but repeated runs with different accuracy have led us to the conclusion that the limit of each limb is indeed a periodic wave.

Notice further, from Fig. 8(a), that there is also a small-amplitude solution with zero phase-shift (as there must be in the limit of small ε according to Theorem 2.1). In fact, the solution depicted in Fig. 7(b) asymptoting to the smallest periodic orbit is the zero-phase-shift orbit occuring towards the bottom of the right-hand limb in Fig. 8(a). Recall that the near circular orbit in that figure also occurs with (almost) zero phase shift.

In Figs. 8(c)–(d) we have plotted the analogue of Fig. 8(a) for three further values of ε. Note that all four pictures are qualitatively the same, but that the minimum amplitude of periodic orbits for which there exists a homoclinic orbit decreases with ε. This observation, sheds more light on the paradox, mentioned in Section 2, that there are no homoclinic orbits to zero but there are homoclinic orbits to periodic orbits with arbitrary small amplitude as $\varepsilon \to 0$. Namely, for finite ε, there do not exist homoclinic orbits to periodic

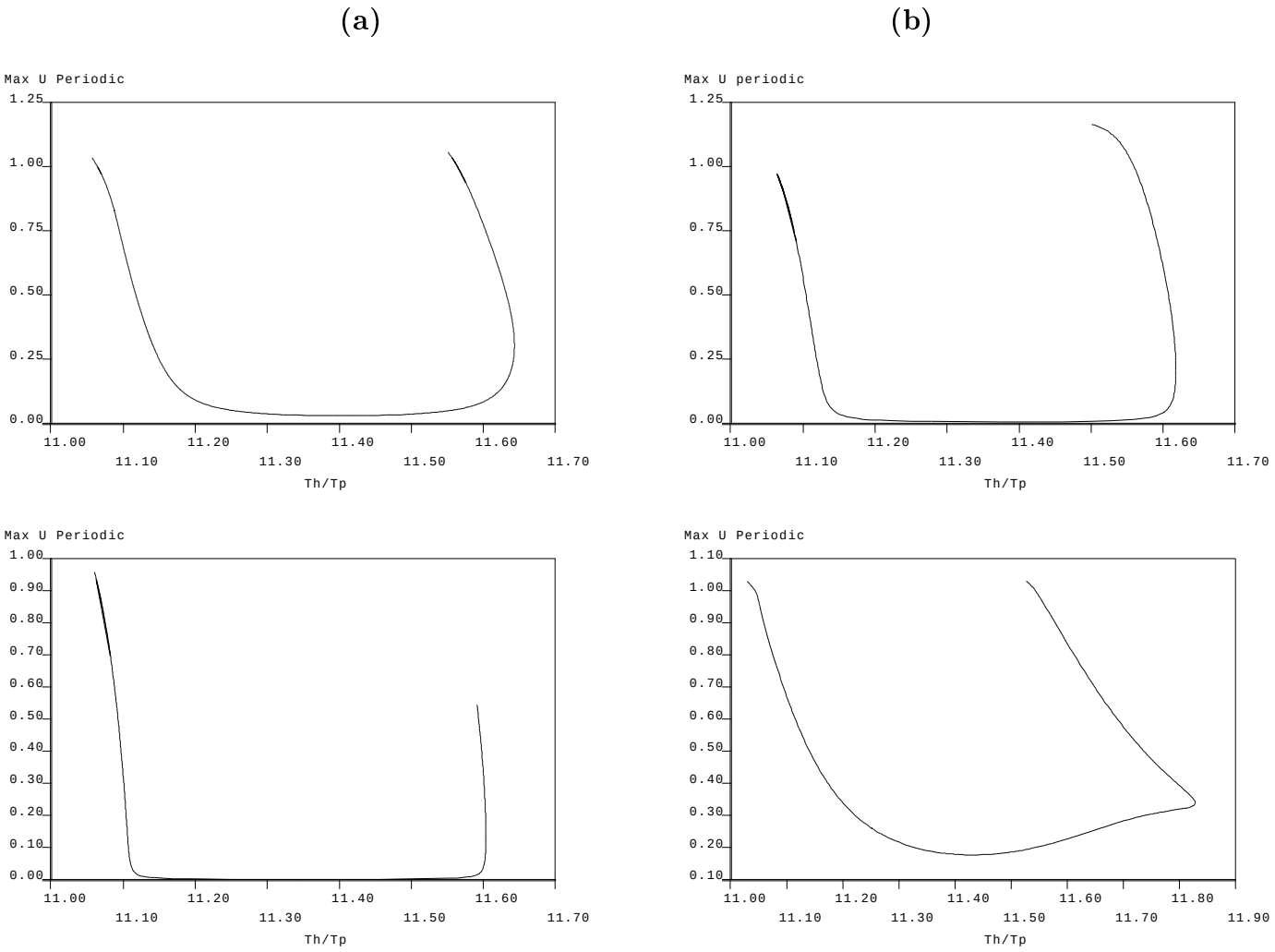

Figure 8: Loci of homoclinic solutions to periodic orbits for (a) $1/\varepsilon^2 = 10$, (b) $1/\varepsilon^2 = 15$, (c) $1/\varepsilon^2 = 20$ and (d) $1/\varepsilon^2 = 3.48$. The x–axis corresponds to phase-shift and the y-axis measures the amplitude of the periodic orbit (see text for details).

orbits of arbitrary small amplitude. We note also from the statement of Theorem 2.1 that there should be a connection to small amplitude orbits for all phase-shifts in $[0, 1]$, appears to be satisfied by the U-shaped curve becoming increasingly square as $\varepsilon \to 0$ with the bottom of the U filling out the required interval of phase-shifts (recall again that the phase-shift is twice the non-integer part of T_H/T_P in Fig. 8. Further conjectures about the behaviour with ε of solutions with different phase-shifts are presented in the conclusion section which follows.

To probe the behaviour on varying ε more carefully, we have performed continuation of homoclinic orbits as ε varies, with either the phase-shift or the Hamiltonian value fixed. We present first the results on continuation with fixed H, with T_H/T_P allowed to vary. Fig. 9 shows an example of such a computation. Note first that the period of the amplitude and periods of the orbit scale with ε, in agreement with (2.1) and the functional form of H (1.2). Secondly, note from that the phase shift T_H/T_P appears to settle down to a constant value as $\varepsilon \to 0$, which is consistent with the orbit belonging to part of a vertical limb of the amplitude-versus phase-shift plot as $\varepsilon \to 0$. Finally, note that we should not expect to see exponential scaling of the amplitude of periodic obit, since, by taking H constant we *a priori* fix the periodic orbit.

Next we follow orbits of fixed phase-shift, by fixing the ratio of T_H to T_P and allowing ε and the Hamiltonian H to vary. We present results first for a homoclinic solution to small amplitude periodic orbit with fixed phase shift $P_H = 0.5$. Fig. 10(a) & (b) shows the amplitude of the periodic orbit plotted against $\eta = 1/\varepsilon^2$. Here there is strong evidence of the exponential scaling of Theorem 2.1 occuring. More precisely, Fig. (10)(b) suggests that

$$\text{amplitude } \sim \varepsilon^2 \exp(1/\varepsilon) \quad \text{as} \quad \varepsilon \to 0, \tag{4.1}$$

which scaling was suggested by the asymptotic analysis of Grimshaw & Joshi (1995). Fig. 11 shows the analogue of Fig. 10(a) and (b) for several values of the phase shift including the small amplitude zero phase-shift solution depicted in Fig. 7(b). It is evident that the scaling (4.1) is satisfied for each phase shift and, moreover, that for small ε the zero-phase-shift solution has larger amplitude than the non-zero cases. This figure is discussed further in the concluding section.

4.2 Multi-modal solutions

In Section 2.3 we argued that multi–modal homoclinic solutions to periodic orbits for equation (1.1) should exist under a transversality assumption. We have been able to compute many symmetric multi-modal solutions using the shooting technique mentioned at the end of Section 3. For reasons of brevity, we present only three; Fig. 12 depicts a symmetric tri–modal solution for $\varepsilon \approx 0.2402$ ($\eta = 17.33221$) and Figs. 13 and 14 show qualitatively distinct symmetric 5–modal solutions for $\varepsilon \approx 0.2365$ ($\eta = 17.87877$) and $\varepsilon \approx 0.2377$ ($\eta = 17.69871$) respectively. The fact that we have been able to compute these multi–modal solutions is strong *a posteriori* evidence for the existence of a transverse intersection of the stable and unstable manifolds as discussed in Section 2.3.

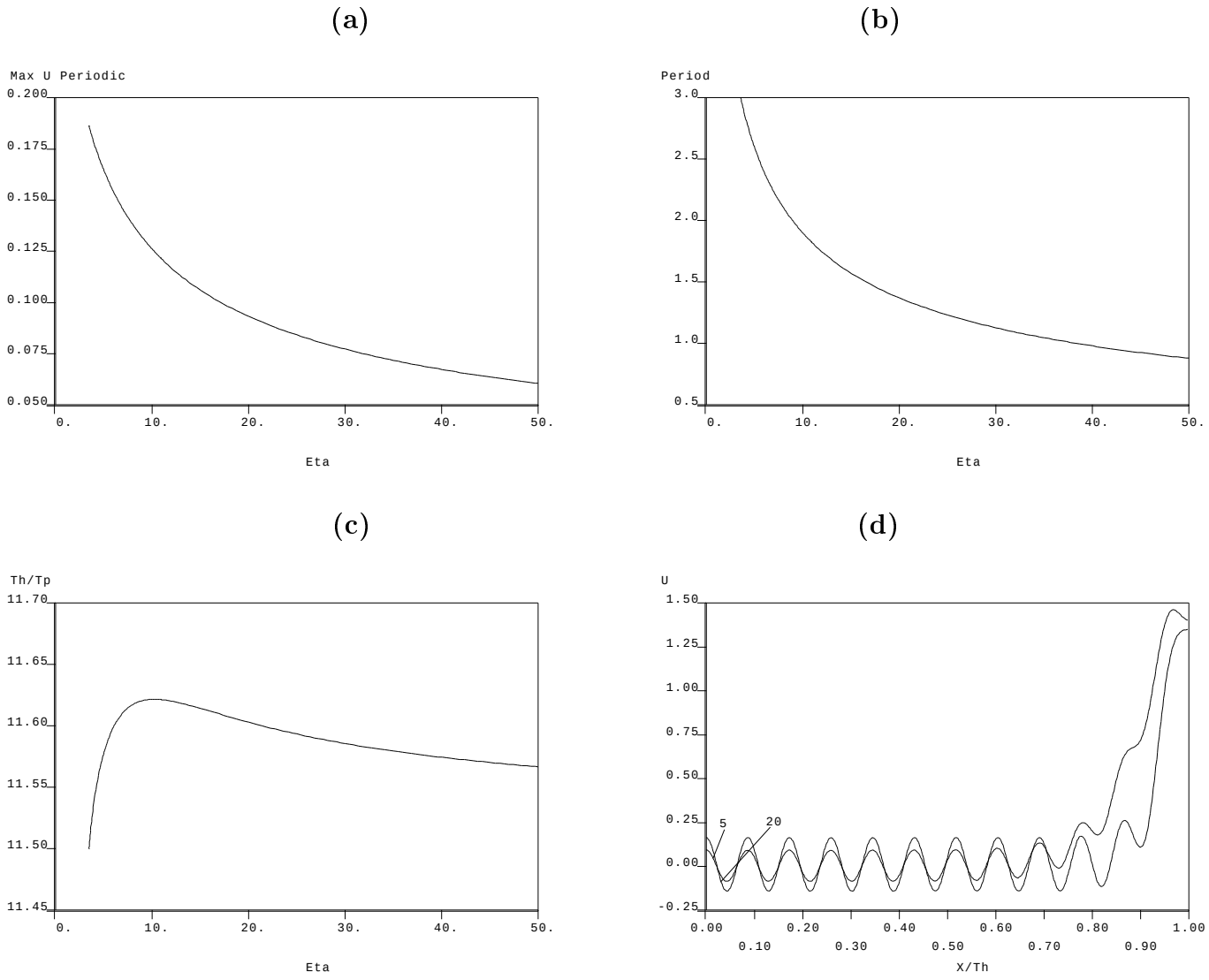

Figure 9: Branch of homoclinic solutions to periodic orbits with fixed $H = -9.1544 \times 10^{-2}$ as $\eta = 1/\varepsilon^2$ varies; (**a**) amplitude of periodic orbit versus η, (**b**) period versus η. (**c**) T_H/T_P versus η, (**d**) Two solutions on the branch for $\eta = 20$ and $\eta = 5$.

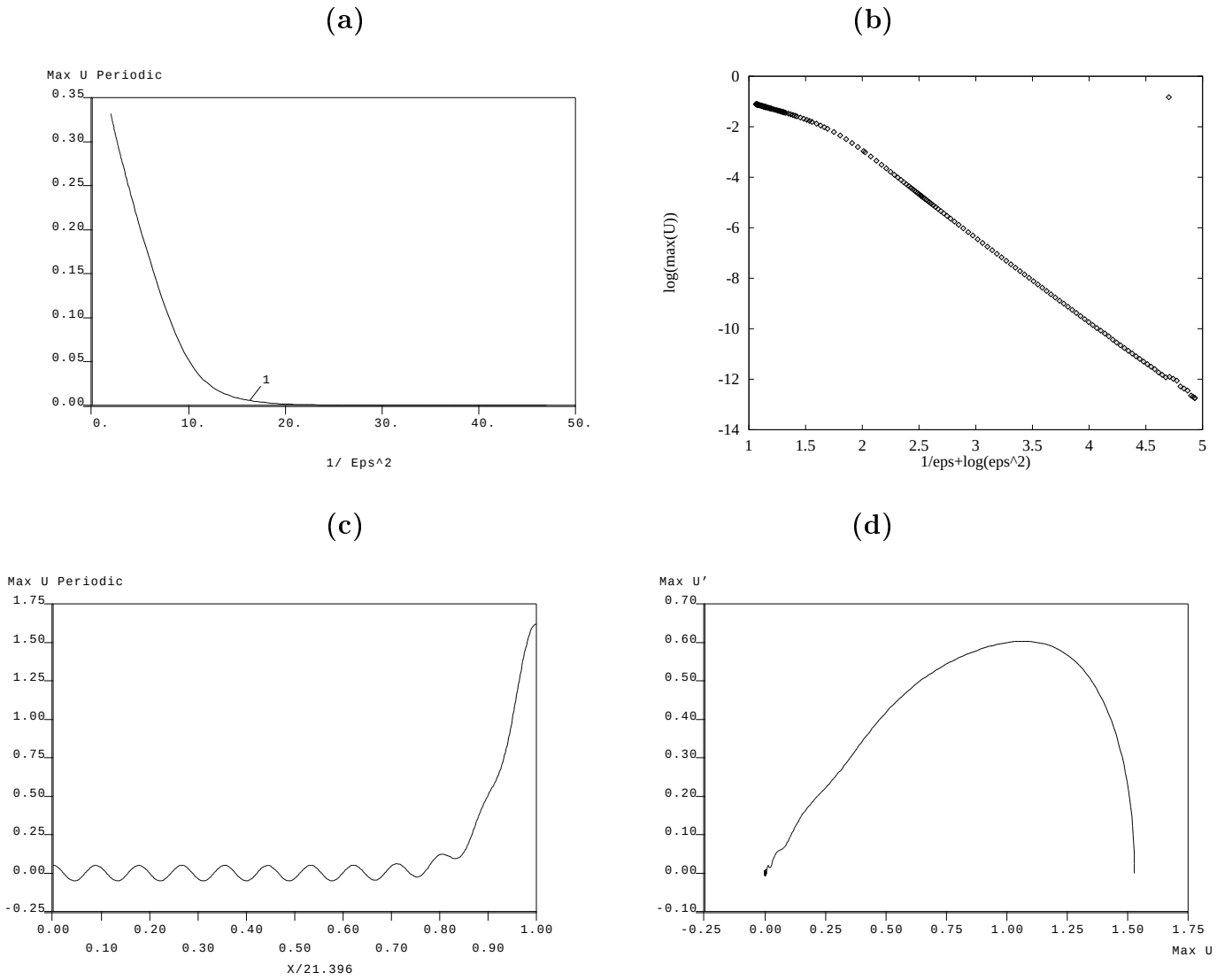

Figure 10: (**a**) Branch of homoclinic solutions to periodic orbits for fixed phase-shift $P_h = 0.5$, as ε varies, plotted as the amplitude of the periodic orbit against η. (**b**) A portion of the same branch plotted on a certain logarithmic scale. (**c**),(**d**) Solutions on the branch for (**c**) $\eta = 10.0$ and (**d**) $\eta = 20.0$.

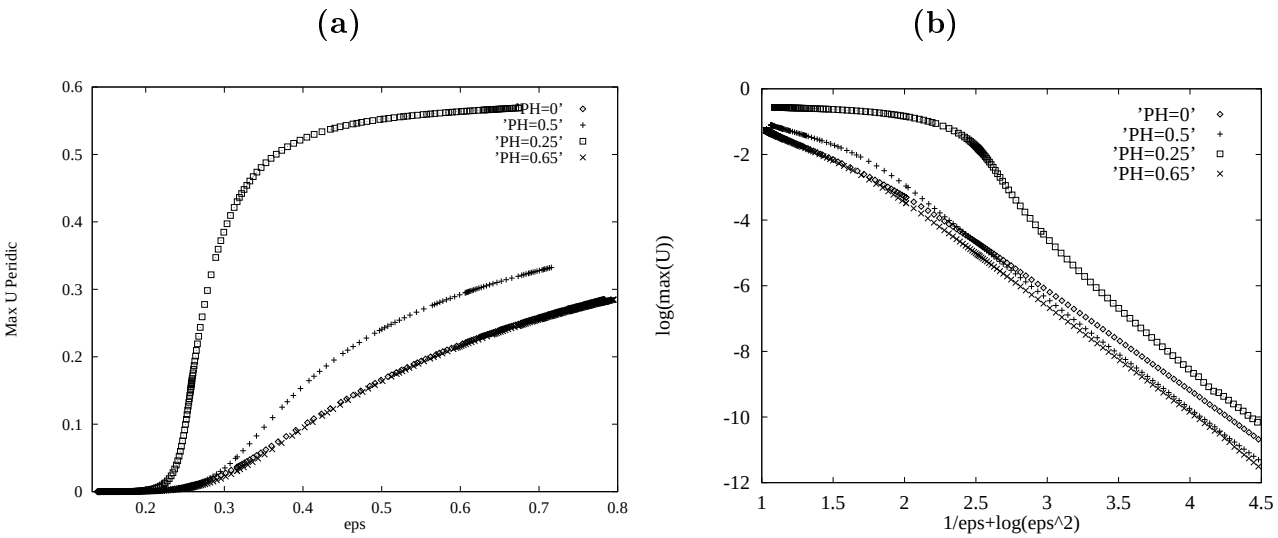

Figure 11: (**a**) A portion of the branch of homoclinic solutions to periodic orbits for fixed phase-shifts $P_H = 0, 0.25, 0.5, 0.65$ plotted as the amplitude of the periodic orbit against ε. (**b**) The same information plotted on a certain logarithmic scale.

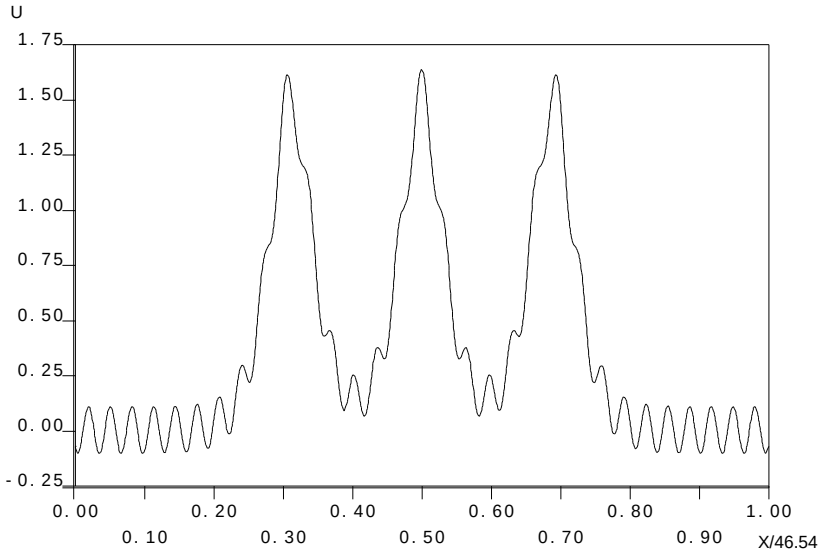

Figure 12: A tri–modal solution for $\varepsilon \approx 0.2402$

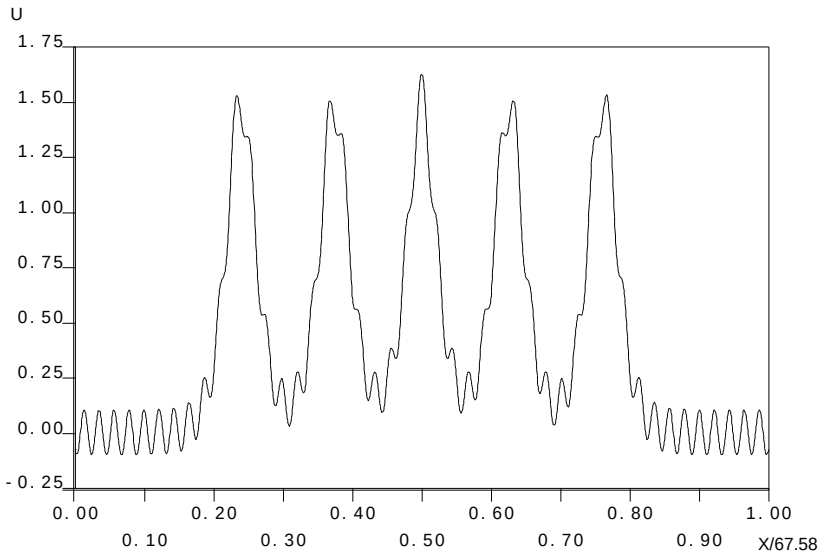

Figure 13: A 5–modal solution for $\varepsilon \approx 0.2365$

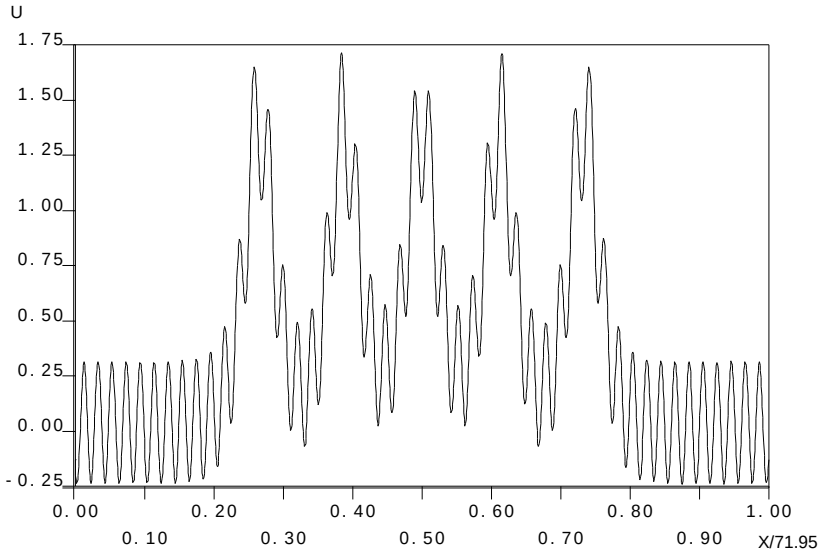

Figure 14: A 5–modal solution, $\varepsilon \approx 0.2377$

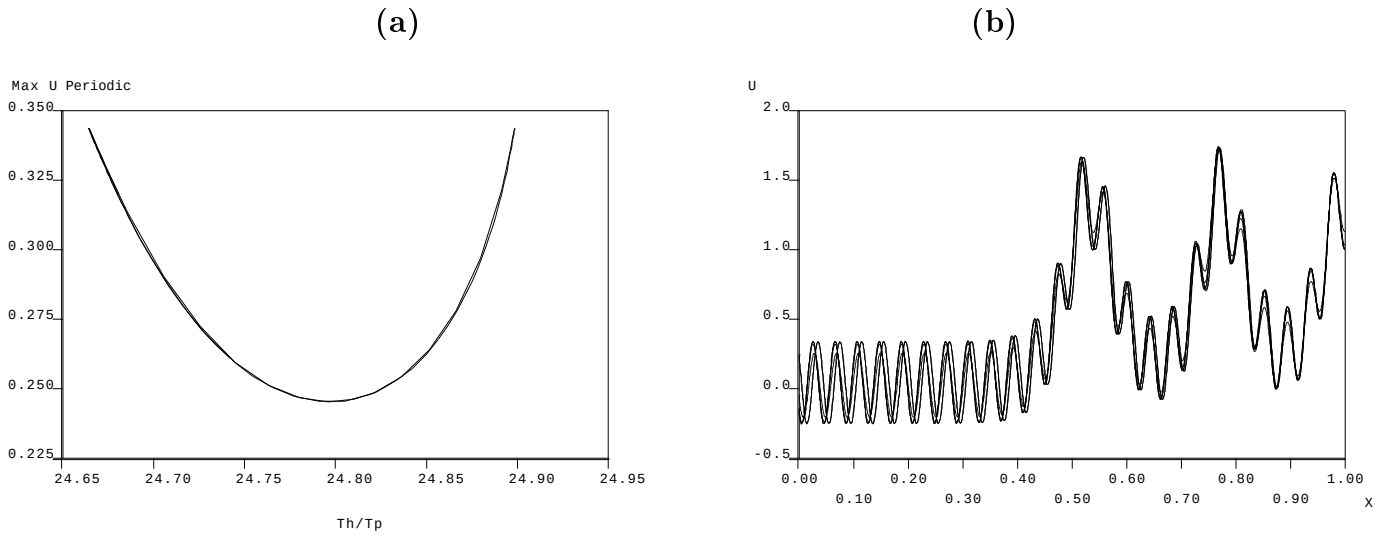

Figure 15: (**a**) Locus of 5-modal solutions for fixed $\varepsilon \approx 0.2365$ as phase-shift against amplitude of periodic orbit. (**b**) Multi–modal solutions on the branch, for different phase-shifts.

As was the case for the uni–modal homoclinic orbits to periodic orbits, we have been able to investigate the global behaviour of multi–modal solutions both for fixed ε as the phase shift and periodic orbit vary, and as ε varies. To illustrate these continuation procedures we present results only for the 5–modal solution of Fig. 13 which we expect to be indicative of the global behaviour of other multi-modal solutions. Fig. 15 depicts the results of continuation of the solution for fixed ε allowing P_H and the Hamiltonian H to vary. In contrast to the situation for uni–modal solutions, the branch of solutions was found to be an iosola with limit points at $P_H \approx 0.34$ and $P_H \approx 0.78$ so that neither the zero-phase-shift nor the large-amplitude limit were approached. These findings are best illustrated in Fig. 15(a) in which the two branches of solutions between the two limit points are almost overlaid.. Fig. 15(b) plots three solutions on the branch for different phase-shift values.

Fig. 16(a) shows the results of continuation of the solution in Fig. 13 with respect to ε where the phase-shift was fixed and the Hamiltonian H was allowed to vary. There are several points of interest on this graph. First we note there are two branches, an upper and lower branch, emanating from the point $\eta = 17.81839$ which was, in fact, detected to be a turning point. The two branches then coalesce at another turning point given at $\eta = 4.44476$, the global curve forming an iosola. The solution for $\eta = 17.81839$ is qualitatively similar that plotted in Fig. 13, which is on the lower of the two branches marginally away from the turning point. Fig. 16(b) depicts the solution at the turning point at $\eta = 4.44476$. There are two further turning points: one on the upper branch for $\eta = 2.03538$ and one on the lower branch for $\eta = 2.13782$, the solution at the latter is plotted in Fig. 16(c). Finally, Fig. 16(d) depicts two solutions from the upper branch at $\eta = 3.1$ and $\eta = 17.4$. All these solutions are depicted on the half-interval up to the point of symmetry.

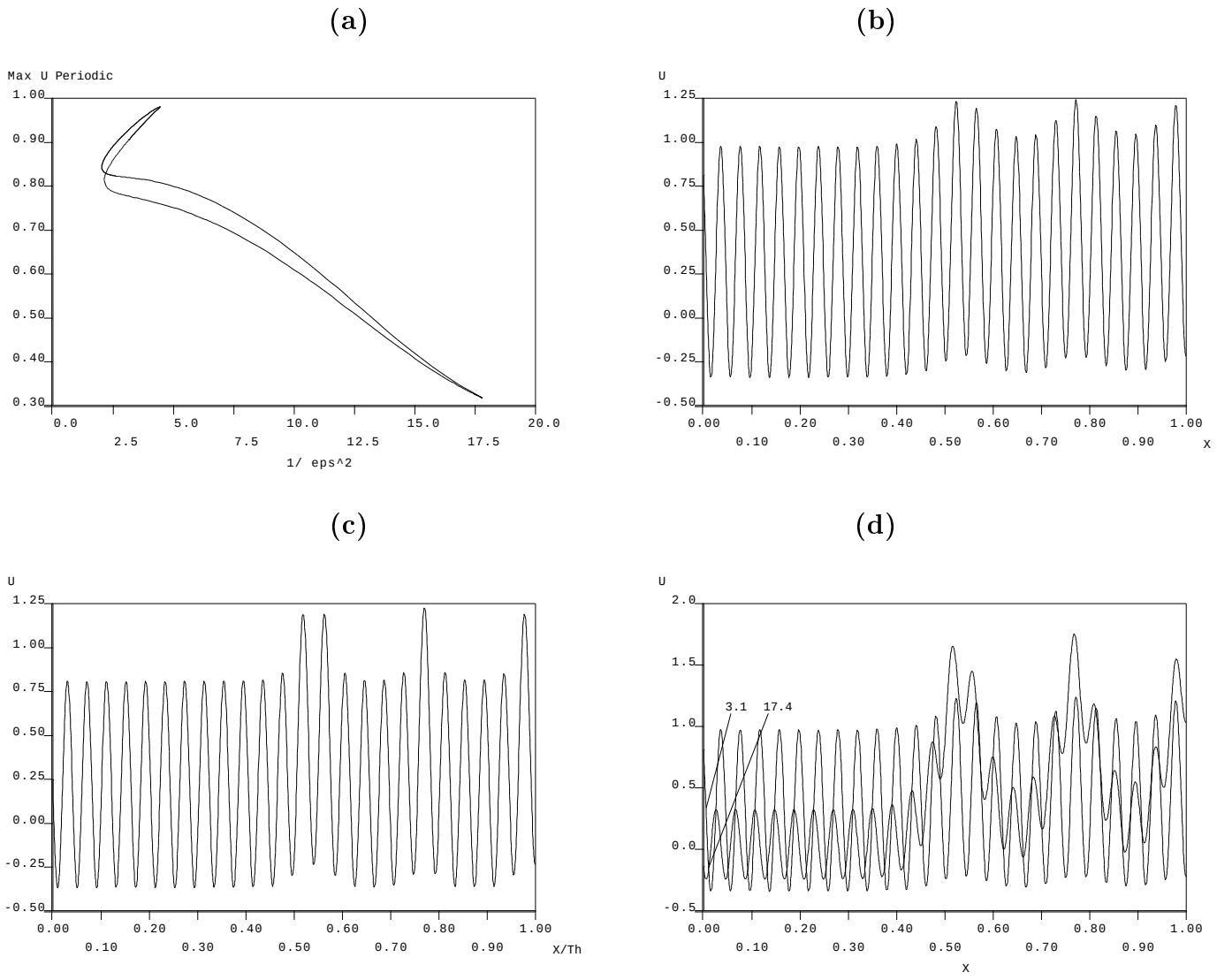

Figure 16: (**a**) Global bifurcation diagram of a branch of 5-modal homoclinic orbits to periodic orbits as ε varies, (**b**) solution at the turning point at $\eta = 4.44476$, (**c**) solution at the turning point on lower branch at $\eta = 2.13782$ and (**d**) two solutions on the upper branch for $\eta = 3.1$ and $\eta = 17.4$.

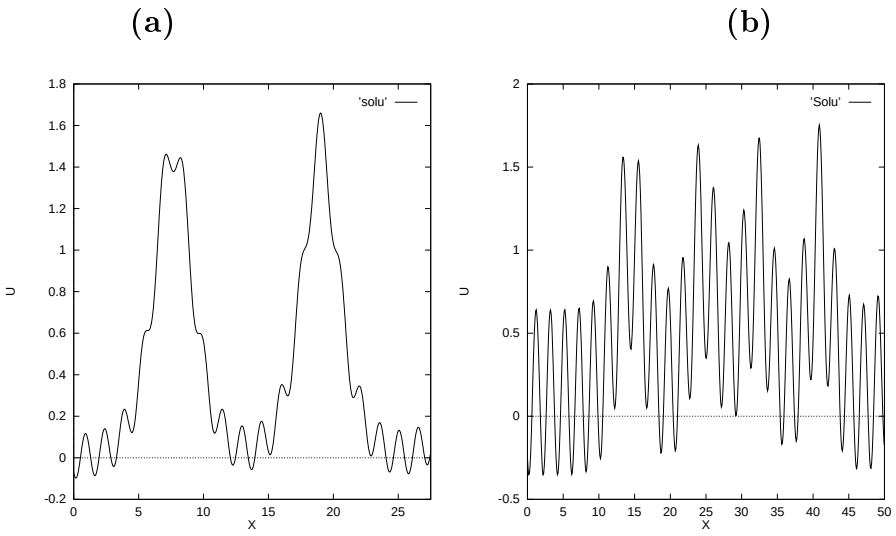

Figure 17: Two examples of non–symmetric solutions to (1.1), (**a**) $\eta = 17.33517$, and in (**b**) $\eta = 9.16992$.

Thus far all computed solutions to (1.1) have been symmetric, although the multi-modal orbits suggested by the arguments in Section 2.3 are not restricted to this class. To illustrate this, in Fig. 17 we present two examples of non–symmetric multi–modal solutions for two different values of ε. We have found numerical evidence for the existence of many more asymmetric solutions.

Conclusion

In this paper we have demonstrated a quite general numerical method for the continuation of homoclinic solutions to periodic solutions for Hamiltonian systems, and its simplification in the special case of a reversible system.

This numerical method was applied to the model Hamiltonian problem (1.1), which is of interest because of its connection with the gravity-capillary water-wave problem and the fifth-order KdV equation (1.3). A key contribution has been to further resolve the apparent paradox that solutions homoclinic to arbitrarily small periodic orbits have been proved to exist, but that homoclinic orbits to zero have been proved not to exist. The resolution lies in first realising, as argued in Section 2.2, that the two forms of solution have different codimension. Then, the numerical results in Fig. 8 indicate that the key is that for fixed $\varepsilon > 0$ there do not exist homoclinic solutions to arbitrarily small periodic orbits, but that the arbitrary smallness comes only in the limit $\varepsilon \to 0$, in which singular limit there does exist a homoclinic orbit to the origin. We recall that for the full water-wave problem, in which there are two independent parameters, the existence of homoclinic orbits to the zero solution remains an open problem for the parameter regime corresponding to (1.1).

We have also been able to extend the analytical results of Amick & Toland (1992) to large-amplitude solutions. It appears that for each ε there exist homoclinic solutions

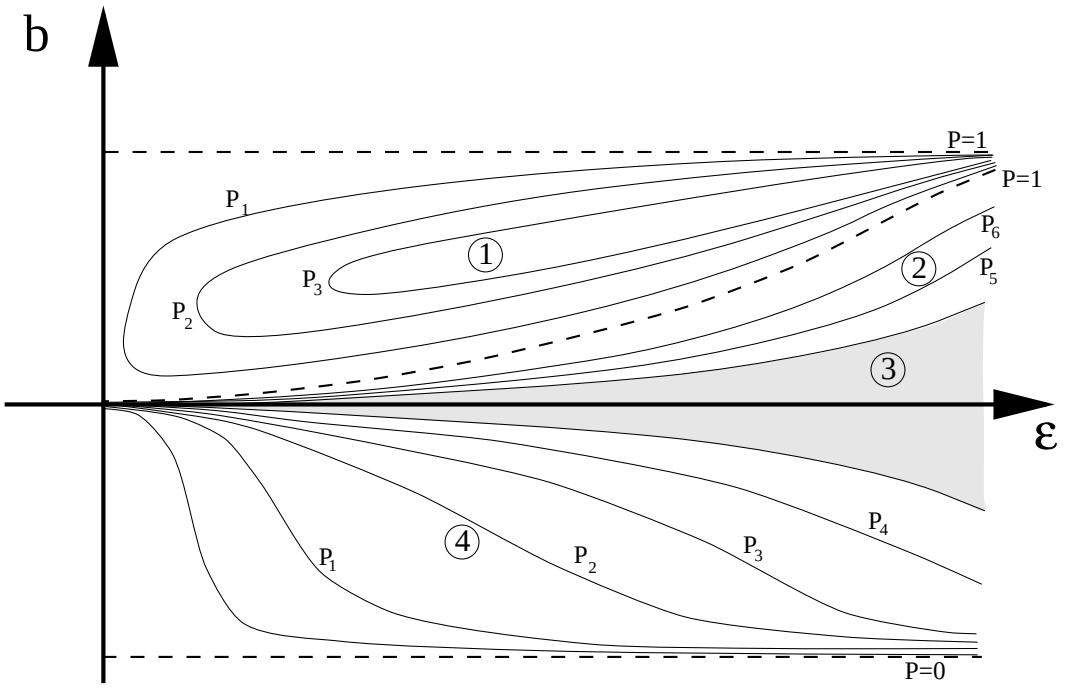

Figure 18: Conjectured plot showing loci of homoclinic orbits of fixed phase-shift against ε and b. Dashed lines represent the case of zero phase-shift $P_H = 0 (\mathrm{mod}\, 1)$. The other annotated are indicative and are assumed to ordered according to $0 < P_1 < \ldots < P_6 < 1$. The shaded region (3) represents periodic orbits for which there is no homoclinic connection (this is *not* the same as the shaded region in Fig. 1). See text for explanation of other region numbers.

to large-amplitude periodic orbits with the locus of homoclinic orbits forming a characteristic asymmetric U-shape in phase-shift versus amplitude (Fig. 8). The limiting large-amplitude solution is a pure periodic orbit. We have also paid particular attention to zero phase shift solutions which formed a special case in the analysis. The reason for this being a special case can be explained from our results. We conjecture that in the limit $\varepsilon \to 0$, zero phase shift corresponds exactly to a vertical wall of the U-shaped curve.

In Fig. 18 we present a conjecture for the uni-modal homoclinic solutions to periodic orbits of fixed phase-shift, based on the numerical results contained in Figs. 8, 10 and 11. We have plotted the "contour map" of fixed phase shift in the (ε,b) plane, where b measures the amplitude of periodic solutions (as in (2.1)) Care has to be taken in interpreting this diagram. Recall that periodic solutions with $b < 0$ are identified with those for $b > 0$ via translation through half a period. Thus, for fixed ε, the two points on the boundary of region 3 represent the same homoclinic solution. Region 3 corresponds to periodic solutions to which there do not exist homoclinic orbits. Note that the width of this region is exponentially thin as $\varepsilon \to 0$. The two dashed horizontal lines (denoted P=0 and P=1) in the figure represent the large-amplitude zero-phase-shift periodic orbit that is reached upon varying P for fixed ε (c.f. Fig. 8). The other identified curve of zero-phase-

shift periodic orbits corresponds to those proved to exist according to Theorem 2.1. All other orbits described by the theorem occur between this curve and the lower horizontal line (regions 2 and 4). Curves in region 1, which form limit points with respect to ε, are not covered by Amick & Toland's theory. Finally we observe that for all periodic orbits not in region 3, there exist two distinct homoclinic orbits with different phase shifts.

Another important new result is the strong evidence we have presented for the existence of *multi–modal* homoclinic solutions to periodic orbits for (1.1), via generic reasoning and explicit computation. Indeed, we have been able to compute both symmetric and asymmetric solutions. The existence of the latter would disprove a conjecture of Boyd (1991)[p 145] that only symmetric solutions should exist (although clearly Boyd had in mind only uni-modal solitary-waves). The global behaviour of one branch of multi-modal solutions was examined in detail and showed to undergo limit points with respect to a parameter (*coalescences* in the parlance of Buffoni et al. (1994)). We note the significance of coalescences in the context of the underlying infinite dimensional problem, that they would typically correspond to an eigenvalue crossing through zero, and hence to a change of the stability property of the branch. Apart from this simple comment, we know of no other information concerning the stability or otherwise of the solutions we have computed for either (1.3) or the full water-wave problem.

Clearly our results only scratch at the surface of understanding the global existence properties of homoclinic orbits to periodic orbits of (1.1). We have computed the branch of only one multi-modal orbit in detail, which we nonetheless hope to be indicative of others. Recall however, that for *each* unimodal orbit for which we can prove transversality, there must be infinitely many multi-modal orbits, for all ε. The fact that the computed multi-modal underwent a limit-point and could not be computed to arbitrary small ε does not provide a contradiction. Indeed, by analogy with the case in (Buffoni et al. 1994), we would expect that as ε decreases only multi-modal solutions with an increasingly large number of oscillations between each hump should exist. Further numerical experiments are required in order to get a more complete picture. We also mention that we expect *each* orbit homoclinic to a periodic orbit to have a one dimensional continuum of periodic orbits associated with it, for which the homoclinic orbit arises as the infinite-period limit (*cf.* the periodic solutions computed in Boyd (1991)[Fig. 2]).

There follow some comments about the reliability of our numerical results. Although we know of no error analysis for the numerical continuation method, we know that it is well-posed (Beyn 1994) and that the projection boundary conditions give the best possible linear boundary conditions (Beyn 1990). However, we note that great care is required in performing numerics approaching the singular limit since it is easy to compute spurious solutions. For this reason, we do not wish to claim that all the results we present are necessarily quantatively correct. However, we do believe that the results provide a coherent picture of the global behaviour homoclinic orbits to periodic orbits for (1.1). Taken in this spirit, we hope that the present paper will provide a stimulus for further rigourous results in the future.

Despite these reservations, there appears to be good agreement (Figs. 10 and 11) with the asymptotic results of Grimshaw & Joshi (1995) which show the scaling (4.1) of the

amplitude of periodic orbits to which homoclinic orbits occur. Note also that Grimshaw and Joshi's results predict a (symmetric) U-shaped curve as in Fig. 8. We have recently become aware of further asymptotic results by Sun (1996) which appear to also predict the observed asymmetry in the U-shaped curves. A careful comparison between our results and the asymptotic theory is left for future work.

As mentioned in the introduction, Boyd (1991) provides a list of applications of homoclinic orbits to periodic orbits arising in applications. The fields of application cover meteorology, plasma physics, oceanography and particle physics in addition to hydrodynamics. It is to be expected that the numerical techniques outlined in this paper may be of use in these areas also.

Acknowledgements

The authors are grateful to E. Doedel (Concordia University) for his help in adapting the continuation code AUTO to return the directions associated with the Floquet multipliers. We should also like to thank J.F. Toland (Bath University) for the useful discussions on the theory contained in (Amick & Toland 1992), for commenting on an earlier draft and for suggesting the presentation of our results in the form of Fig. 18. Finally, we thank an anonymous referee for comments which lead to greatly improved accuracy of the computations into the singular limit. GJL is supported by the UK EPSRC.

References

Akylas, T. & Yang, T.-S. (1995), 'On short-scale oscillatory tails of long-wave disturbances', *Stud. Appl. Math.* **94**, 1–20.

Amick, C. & Kirchgassner, K. (1989), 'A theory of solitary water-waves in the presence of surface tension', *Arch. Rational Mech. Anal.* **105**, 1–49.

Amick, C. & McLeod, J. (1991), 'A singular perturbation problem in water-waves', *Stability and Applied Analysis of Continuous Media* **1**, 127–148.

Amick, C. & Toland, J. (1992), 'Solitary waves with surface tension i: trajectories homoclinic to periodic orbits in four dimensions', *Arch. Rat. Mech. Anal* **118**, 37–69.

Bai, F., Lord, G. & Spence, A. (1995), 'Numerical computations of connecting orbits in discrete and continuous dynamical systems', *Int. J. Bifurcation and Chaos.* To Appear.

Beale, T. (1991), 'Solitary water waves with capillary ripples at infinity', *Commun. Pure Appl. Math.* **64**, 211–257.

Belyakov, L. & Shil'nikov, L. (1990), 'Homoclinic Curves and Complex Solitary Waves', *Selecta Mathematic Sovietica* **9**, 219–228.

Beyn, W. (1994), On well-posed problems for connecting orbits in dynamical systems, *in* P. Kloeden & K. Palmer, eds, 'Proceedings of 'Chaotic Numerics', Geelong 1993'.

Beyn, W.-J. (1990), 'The numerical computation of connecting orbits in dynamical systems', IMA *J. Num. Anal.* **9**, 379–405.

Boyd, J. (1991), 'Weakly non-local solitons for capillary-gravity water waves: fifth-degree korteweg-de vries equation', *Physica D* **48**, 129–146.

Buffoni, B., Champneys, A. & Toland, J. (1994), Bifurcation and coalescence of a plethora of homoclinic orbits for a Hamiltonian system, Mathematics Preprint, University of Bath (available by anonymous ftp from *ftp.maths.bath.ac.uk: pub/preprints*).

Buffoni, B., Groves, M. & Toland, J. (1995), A plethora of solitary gravity-capillary water waves with nearly critical bond and froude numbers., To appear in *Phil. Trans. Roy. Soc. London A*: Mathematics Preprint, University of Bath (available by anonymous ftp from *ftp.maths.bath.ac.uk: pub/preprints*).

Champneys, A. & Kuznetsov, Y. (1994), 'Numerical detection and continuation of codimension-two homoclinic bifurcations', *Int. J. Bifurcation & Chaos* **4**, 795–822.

Champneys, A. & Spence, A. (1993), 'Hunting for homoclinic orbits in reversible systems: a shooting technique', *Advances in Computational Mathematics* **1**, 81–108.

Champneys, A. & Toland, J. (1993), 'Bifurcation of a plethora of multi-modal homoclinic orbits for autonomous Hamiltonian systems', *Nonlinearity* **6**, 665–772.

Craig, W. & Groves, M. (1994), 'Hamiltonian long-wave approximations to the water-wave problem', *Wave Motion* **19**, 367–389.

Devaney, R. (1976), 'Reversible diffeomorphisms and flows', *Trans. Amer. Math. Soc.* **218**, 89–113.

Dias, F., Menasce, D. & Vanden-Broek, J.-M. (1995), Numerical study of capillary-gravity solitary waves, Preprint.

Doedel, E. & Kernevez, J. (1986), AUTO: Software for continuation problems in ordinary differential equations with applications, Technical report, California Institute of Technology. Applied Mathematics Technical Report.

Doedel, E., Keller, H. & Kernevez, J. (1991), 'Numerical analysis and control of bifurcation problems: (II) bifurcation in infinite dimensions', *Int. J. Bifurcation and Chaos* **1**, 745–772.

Friedman, M. & Doedel, E. (1991), 'Numerical computation of invariant manifolds connecting fixed points', SIAM *J. Numer. Anal.* **28**, 789–808.

Grimshaw, R. (1995*a*), Solitary waves with oscillatory tails, Applied Mathematics Reports and Preprints 94/28, Monash University.

Grimshaw, R. (1995*b*), 'Weakly nonlocal solitary waves in a singularly perturbed nonlinear Schrödinger equation', *Stud. Appl. Math.* **94**, 257–270.

Grimshaw, R. & Joshi, N. (1995), 'Weakly nonlocal solitary waves in a singularly perturbed Korteweg-de Vries equation', *SIAM J. Appl. Math.* **55**, 124–135.

Guckenheimer, J. & Holmes, P. (1983), *Nonlinear Oscillations, Dynamical Systems and Bifurcations of Vector Fields*, Springer-Verlag, New York, U.S.A.

Haller, G. & Wiggins, S. (1995), 'N-pulse homoclinic orbits in perturbations of resonant Hamiltonian systems', *Arch. Rat. Mech. Anal.* **130**, 25–101.

Homburg, A. J., Kokubu, H. & Krupa, M. (1994), 'The cusp horseshoe and its bifurcations from inclination-flip homoclinic orbits', *Ergodic Theory and Dynamical Systems* **14**, 667–693.

Hunter, J. & Scheurle, J. (1988), 'Existence of perturbed solitary wave solutions to a model equation for water-waves', *Physica D* **32**, 253–268.

Iooss, G. & Kirchgassner, K. (1992), 'Water waves and small surface tension: an approach via normal form', *Proc. Roy. Soc. Edin. A* **122**, 267 –299.

Kirchgassner, K. (1988), 'Nonlinearly resonant surface waves and homoclinc bifurcation', *Adv. Appl. Mech.* **26**, 135–181.

Koltsova, O. & Lerman, L. (1995), 'Periodic orbits and homoclinic orbits in a two-parameter unfolding of a Hamiltonian system with a homoclinic orbit to a saddle-center', *Int. J. Bifurcation Chaos* **5**, 397–408.

Lombardi, E. (1992), 'Bifurcation d'ondes solitaires à oscillation de faible amplitude á l'infini, pour un numobre de froude proche de 1.', *C. R. Acad. Sci. Paris, Sér. 1* **314**, 493–496.

Sandstede, B. (1993), Verzweigungstheorie homokliner Verdopplungen, PhD thesis, Institut fur Angewandte Analysis und Stochastik, Berlin.

Schecter, S. (1995), 'Rate of convergence of numerical approximations to homoclinic bifurcation points', *IMA J. Num. Anal.* **15**, 23–60.

Schmidt, D. S. (1976), Hopf's bifurcation theorem and the center theorem of liapunov, *in* J. Marsden & M. McCracken, eds, 'The Hopf Bifurcation and its Applications', Springer.

Sun, S. (1991), 'Existence of a generalised solitary wave solution for water waves with poitive bond number less than 1/3', *J. Math. Anal Appl* **156**, 533–566.

Sun, S. (1996), 'On the oscillatory tails with arbitrary phase shift for solutions of the perturbed KdV equations'. Preprint: Virginia Polytechhnic Institute and State University.